

Accretion in stellar clusters and the IMF

I. A. Bonnell¹, C. J. Clarke², M. R. Bate² and J. E. Pringle²

¹ *School of Physics and Astronomy, University of St Andrews, North Haugh, St Andrews, Fife, KY16 9SS.*

² *Institute of Astronomy, Madingley Road, Cambridge CB3 0HA.*

5 September 2018

ABSTRACT

We present a simple physical mechanism that can account for the observed stellar mass spectrum for masses $M_* \gtrsim 0.5M_\odot$. The model depends solely on the competitive accretion that occurs in stellar clusters where each star’s accretion rate depends on the local gas density and the square of the accretion radius. In a stellar cluster, there are two different regimes depending on whether the gas or the stars dominate the gravitational potential. When the cluster is dominated by cold gas, the accretion radius is given by a tidal-lobe radius. This occurs as the cluster collapses towards a $\rho \propto R^{-2}$ distribution. Accretion in this regime results in a mass spectrum with an asymptotic limit of $\gamma = -3/2$ (where Salpeter is $\gamma = -2.35$). Once the stars dominate the potential and are virialised, which occurs first in the cluster core, the accretion radius is the Bondi-Hoyle radius. The resultant mass spectrum has an asymptotic limit of $\gamma = -2$ with slightly steeper slopes ($\gamma \approx -2.5$) if the stars are already mass-segregated. Simulations of accretion onto clusters containing 1000 stars show that as expected, the low-mass stars accumulate the majority of their masses during the gas dominated phase whereas the high-mass stars accumulate the majority of their mass during the stellar dominated phase. This results in a mass spectrum with a relatively shallow $\gamma \approx 3/2$ power-law for low-mass stars and a steeper, power-law for high-mass stars $-2.5 \lesssim \gamma \leq -2$. This competitive accretion model also results in a mass segregated cluster.

Key words: stars: formation – stars: luminosity function, mass function – open clusters and associations: general.

1 INTRODUCTION

One of the most fundamental unsolved problems in astronomy is the origin of the distribution of stellar masses, the so-called Initial Mass Function (IMF). Significant observational work has gone into establishing the exact form of the mass spectrum (c.f. Scalo 1986; Kroupa, Tout & Gilmore 1990; Kennicutt 1998) and investigating its universality (Kennicutt 1998; Leitherer 1998; Scalo 1998). Unfortunately this work has not led to an increase in our understanding of how the mass spectrum originates. This shortcoming is intrinsically linked to our lack of understanding of the star formation process. Thus, theories of the IMF have generally involved sufficient free-parameters to ensure that they can reproduce the general form of the mass spectrum but also, unfortunately, ensuring that they do not help us discern the physics involved.

Observations of star forming regions have clearly shown that most stars are formed in clusters (e.g. Lada et al. 1991; Lada, Strom and Myers 1993; Meyer & Lada 1999; Clarke, Bonnell & Hillenbrand 2000). Furthermore, the individual stellar masses found in these clusters span the observed

range of stellar masses and are consistent with being drawn from the field star IMF (Hillenbrand 1997; Hillenbrand & Carpenter 2000). Thus, the basic physics which results in the observed mass spectrum is present in this fundamental building block of the star formation process: the young stellar cluster. Competitive accretion in gas-rich stellar clusters results in a spectrum of stellar masses (Bonnell et al. 1997, 2000) and in this *paper* we investigate whether this process can lead to the observed IMF.

There have been several theories advanced to explain the observed distribution of stellar masses (cf. Clarke 1998; Meyer et al. 2000). These theories generally involve either fragmentation or accretion plus feedback as the basic physics in setting the stellar masses. Fragmentation of a giant molecular cloud can set the stellar mass distribution if the GMC clump-mass distribution is, for some reason, of the same form as the IMF (Elmegreen 1997), or if feedback changes the basic fragment (Jeans) mass (Silk 1977). Alternatively, accretion onto a small isolated protostellar core can set the final masses but this requires a halting mechanism (eg feedback) that really determines the mass distribution (Adams & Fattuzzo 1996). The main criticisms of these theories are

arXiv:astro-ph/0102121v1 7 Feb 2001

that a) they rely on additional processes (e.g. feedback or an initial mass distribution) and b) that they neglect the fact that the stars are not formed in isolation but in clusters and therefore can interact during their formation. Furthermore, they are generally unable to explain why clusters are initially mass-segregated (eg, Hillenbrand & Hartmann 1998; Bonnell & Davies 1998) which should be a requirement of any theory that attempts to explain the IMF. In this *paper*, we discuss how competitive accretion in clusters can set the distribution of stellar masses and result in a mass-segregated cluster.

2 ACCRETION IN CLUSTERS

Young stellar clusters are generally found to contain significant amounts of gas. In fact, the total gas mass is typically many times the mass in stars (Lada 1991). This gas is a remnant of the star formation process and can be understood in terms of the inefficiency of fragmentation where the majority of a system's mass is not immediately included in the fragments but is accreted by them over longer time periods (Larson 1978; Boss 1986; Bonnell & Bastien 1992; Burkert & Bodenheimer 1993; Klessen, Burkert & Bate 1998). This occurs due to the non-homologous nature of gravitational collapse (Larson 1969) so that the amount of mass that has reached the region where and when fragmentation occurs, is small. Thus, the initial fragment mass should generally be small, $M \ll M_{\odot}$. Furthermore, in a cluster environment, the fragment mass, if it is proportional to the Jeans mass, should be smallest in the centre of the cluster where the density is highest, in direct contradiction to the observed mass segregation (Bonnell & Davies 1998; Bonnell et al. 1998). It is thus unlikely that the mass distribution is solely determined by the fragmentation process.

Accretion of the residual gas in clusters can play a crucial role in setting the final stellar masses (Zinnecker 1982; Larson 1992). As all the stars are embedded in the same envelope of gas, they compete for the gas as they move through the cluster. This competition results in unequal mass accretion rates and hence a mass spectrum

Simulations of accretion in small stellar clusters (Bonnell et al. 1997) have shown that even if the stars have equal initial masses, they accrete unevenly with those stars near the centre accreting more than those near the outer parts of the cluster. This dependency of the accretion rates on position in the cluster is even clearer in larger clusters ($N = 100$; Bonnell et al. 2000) where accretion rates can vary by over an order of magnitude from the outside to the cluster centre when the cluster is centrally-condensed. The physics behind this differential accretion is the effect of the cluster potential in funneling material down to the centre plus the individual star's ability to capture this material. Initially uniform clusters also accrete differentially as they evolve towards a centrally-condensed configuration, due to the local competition between stars. The final cluster displays a significant degree of mass segregation due to the differential accretion (Bonnell et al. 2000).

A star's accretion rate depends on its cross section for accreting material, πR_{acc}^2 , the gas density through which it moves, ρ and the velocity with which it moves relative to the gas, V_{rel} :

$$\dot{M}_* = \pi \rho V_{\text{rel}} R_{\text{acc}}^2. \quad (1)$$

The question is what is the accretion radius, R_{acc} . An isolated star of mass M_* , moving in a uniform medium with velocity V_{rel} relative to the gas with sound speed c_s , has an accretion radius given by Bondi-Hoyle accretion where

$$R_{\text{BH}} = 2GM_*/(V_{\text{rel}}^2 + c_s^2) \quad (2)$$

(e.g. Bondi & Hoyle 1944; Ruffert 1996). On the other hand, in a cluster environment where cold gas dominates the potential, the accretion radius can be described by the star's tidal-lobe radius.

$$R_{\text{tidal}} \approx 0.5 \left(\frac{M_*}{M_{\text{enc}}} \right)^{\frac{1}{3}} R, \quad (3)$$

where M_* is the star's mass, M_{enc} is the cluster mass interior to the star's position in the cluster R (e.g. Paczynski 1971; Frank, King & Raine 1985). Material inside this tidal-lobe is more attracted to the star whereas outside this lobe the acceleration is dominated by the cluster potential.

Simulations of accretion in gas-dominated stellar clusters have shown that the accretion is well modelled by a tidal-lobe radius as long as the gas dominates the gravitational potential (Bonnell et al. 2000). When this is the case and the gas is unsupported, as expected in order for the cluster to have fragmented, both the gas and the stars collapse towards the cluster centre. The stars are impeded from virialising due to the changing potential, and the gas accretion. Therefore the gas and stellar velocities are locally correlated such that the relative gas velocity is small. This results in a large R_{BH} such that $R_{\text{BH}} > R_{\text{tidal}}$ and therefore the smaller R_{tidal} is the appropriate accretion radius.

In contrast, once the stars dominate the gravitational potential, which occurs first in the core of the cluster due to the higher accretion rates there and the sinking of the more massive stars, the stars virialise and their velocities relative to the gas become large. When this occurs the Bondi-Hoyle radius becomes much smaller due to the large gas velocities such that $R_{\text{BH}} < R_{\text{tidal}}$. At this point, the Bondi-Hoyle radius is a better description of the accretion radius (Bonnell et al. 2000).

3 THE INITIAL MASS FUNCTION

In order to use the above formulations of the accretion rate to determine the resultant mass spectrum, we need a basic model of a stellar cluster. The cluster is initially gas dominated in order to provide the mass reservoir for accretion. Observations of the youngest clusters estimate that up to 90 per cent of the mass is in gas (Lada 1991). Such systems are unlikely to be in equilibrium, and regardless of their initial configurations, will collapse towards a

$$\rho \propto R^{-2} \quad (4)$$

density distribution (Larson 1969; Hunter 1977). The stars will also collapse, even if initially virialised, due to the change in the potential. Thus we assume that the stars follow the same distribution:

$$n \propto R^{-2} \quad (5)$$

This profile is a good approximation to the stellar distribution of most clusters (Binney & Tremaine 1987) including

the youngest clusters that have been studied such as the Orion Nebula cluster (Hillenbrand & Hartmann 1998). Furthermore, it is the expected distribution produced by a violent relaxation of a non-equilibrium purely stellar cluster (Lynden-Bell 1967).

The gas distribution will be modified by the accretion and hence removal of material. The accretion rates are largest in the centre and hence it is there that they will first affect the density profile. This gas removal destabilises the equilibrium of the isothermal sphere allowing gas to infall from further out in the cluster. In the case of infall onto a point-mass, the density profile then takes on the form (Hunter 1977; Shu 1977; Foster & Chevalier 1993)

$$\rho \propto R^{-\frac{3}{2}}. \quad (6)$$

We thus assume an initial density profile of an isothermal sphere (equation 4) which evolves towards a profile composed of the shallower, equation(6) profile in the central regions while the outside maintains the isothermal sphere profile. The transition between these two regimes occurs when gas accretion has increased the stellar masses sufficiently that the stars dominate the gravitational potential in the cluster centre. We discuss the asymptotic limits to the accretion and mass spectrum in these two cases below.

3.1 Gas dominated potentials

In addition to the gas density we require estimates of the relative gas velocity and of the accretion radius. Where gas dominates the potential ($\rho \propto R^{-2}$), the accretion radius is given by the tidal-lobe radius (Bonnell et al. 2000)

$$R_{\text{acc}} \approx R_{\text{tidal}}. \quad (7)$$

In order to evaluate the tidal-lobe radius we need the mass enclosed at a particular radius in the cluster, R ,

$$M_{\text{enc}} = \int_0^R 4\pi\rho r^2 dr, \quad (8)$$

which in a $\rho \propto R^{-2}$ distribution is

$$M_{\text{enc}} \propto R. \quad (9)$$

Simulations of accretion in stellar clusters have shown that in gas-dominated clusters, the relative gas velocity is generally subsonic as both the stellar and gas velocities are dominated by the acceleration of the cluster potential (Bonnell et al. 2000). Alternatively, if the stars are virialised then the relative gas velocity is the velocity dispersion,

$$V_{\text{rel}} \approx \sqrt{\frac{GM_{\text{enc}}}{R}}, \quad (10)$$

Thus, if the gas distribution follows equation(4), then we have

$$V_{\text{rel}} = \text{constant}. \quad (11)$$

In either case the relative gas velocity is independent of position in the cluster.

We can now use the above to consider how accretion in a stellar cluster results in a mass spectrum of the form

$$dN \propto M_*^\gamma dM_* \quad (12)$$

where $\gamma = -2.35$ is the Salpeter IMF. First of all, we note that from equation(5) the number of stars at a given radius is constant:

$$dN = n(R)4\pi R^2 dR \propto \text{const} \times dR. \quad (13)$$

Starting from the general equation for the accretion rates,

$$\dot{M}_* = \pi\rho V_{\text{rel}} R_{\text{acc}}^2, \quad (14)$$

and adapting it for the case where gas dominates the potential such that $\rho \propto R^{-2}$ and $R_{\text{acc}} \approx R_{\text{tidal}}$, then we have

$$\begin{aligned} \dot{M}_* &\propto g(t)R^{-2} \times \left(\left[\frac{M_*}{M_{\text{enc}}} \right]^{\frac{1}{3}} R \right)^2 \\ &\propto g(t) \left(\frac{M_*}{M_{\text{enc}}} \right)^{\frac{2}{3}} \\ &\propto g(t) \left(\frac{M_*}{R} \right)^{\frac{2}{3}}. \end{aligned} \quad (15)$$

The term $g(t)$ includes all time-dependence of the homologically evolving cluster and R is the initial stellar position in the cluster.

Integrating equation(15) with respect to time, t , and in the limit where accretion dominates the final mass, we get

$$M_* \propto R^{-2} h(t)^3, \quad (16)$$

where $h(t) = \int g(t) dt$. Thus, at a time t_{final} , when the accretion is halted, we have

$$R \propto M_*^{-\frac{1}{2}} \quad (17)$$

and thus

$$dR \propto M_*^{-\frac{3}{2}} dM_*. \quad (18)$$

This results in a mass spectrum (equation 13)

$$dN \propto M_*^{-\frac{3}{2}} dM_*. \quad (19)$$

In general, the $\rho \propto R^{-2}$ profile will not extend right to the centre of the cluster. Instead, the central regions must have a flatter profile to stop the density from becoming infinite. A collapsing isothermal gas cloud has a $\rho \propto R^{-2}$ density profile in the outer regions and an ever decreasing central region with near uniform density (Larson 1969). Stars in this region will see a shallower density profile which will affect their accretion rates (equation 14). Adapting equation(15) for a density profile $\rho \propto R^{-\alpha}$ while maintaining a uniform V_{rel} gives

$$M_* \propto R^{-\alpha} \quad (20)$$

and analogous to equation(18),

$$dR \propto M_*^{-\frac{1}{\alpha}-1} dM_*. \quad (21)$$

Taking the stellar density to be proportional to the gas density, $n(R) \propto \rho(R)$, equation(13) becomes

$$\begin{aligned} dN &= n(R)4\pi R^2 dR \propto R^{2-\alpha} dR, \\ &\propto M_*^{-\frac{2}{\alpha}} M_* M_*^{-\frac{1}{\alpha}-1} dM_*, \\ &\propto M_*^{-\frac{3}{\alpha}} dM_*, \end{aligned} \quad (22)$$

and γ is now $\gamma = -3/\alpha$. From equation(22) we see that when the density profile is shallower than R^{-2} , the resulting mass spectrum is steeper than $M_*^{-3/2}$. Figure 1 plots the resulting IMF using equation(22) and a density profile that combines an outer region with a $\rho \propto R^{-2}$ profile with an inner Gaussian density profile (fitted onto the outer region

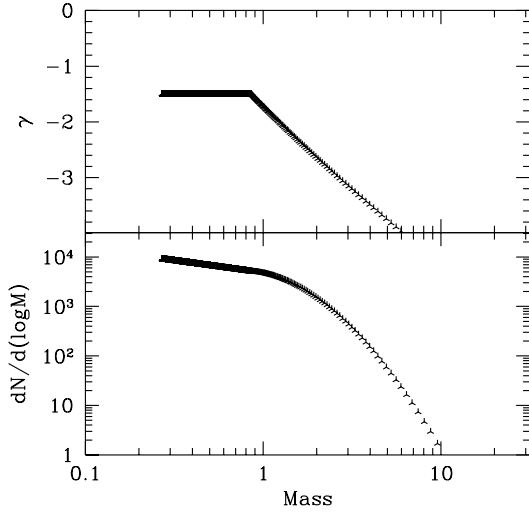


Figure 1. The resultant IMF as derived from equation(22), is plotted in log mass bins for a gas dominated cluster with $\rho \propto R^{-2}$ on the outside and a Gaussian central density profile (lower panel). The masses are scaled such that the average mass is $0.4M_{\odot}$. The upper panel shows the corresponding value of γ where $dN = M_{*}^{\gamma} dM_{*}$. The lower-mass stars have a $\gamma = -3/2$ ($\Gamma = -1/2$) mass spectrum (where Salpeter is $\gamma = -2.35$) due to the $\rho \propto R^{-2}$ whereas the more massive stars have an ever steepening mass spectrum due to the central Gaussian density profile (upper panel).

where it has the same slope). The mass spectrum is plotted as a function of the logarithm of the mass such that the slope is $\Gamma = \gamma + 1$. The low-mass stars that form in the outer region have the $\gamma = -3/2$ mass spectrum whereas the higher-mass stars formed in the inner regions have an ever steeper mass spectrum due to the central Gaussian density profile that converges to uniform density. It is also worth noting that if the collapse gives a density profile that is steeper than R^{-2} as was found in the outer regions of the collapse of a Bonnor-Ebert spheroid (Foster & Chevalier 1993), then this translates (equation[22]) into a shallower IMF for the low-mass stars that are in this region.

3.2 Stellar dominated potentials

In contrast to a gas dominated system, when the cluster potential is dominated by the stars and they are virialised, the appropriate accretion radius is the Bondi-Hoyle radius (Bonnell et al. 2000). The Bondi-Hoyle radius models better the accretion radius as the gas and stellar velocities are no longer correlated. The gas is primarily infalling from further out in the cluster onto the stellar dominated core. When infall is onto a point mass, the resulting velocity profile is

$$V_{\text{rel}} \propto R^{-1/2} \quad (23)$$

which assuming a constant mass infall rate with radius implies a density profile of the form of equation(6),

$$\rho \propto R^{-3/2}. \quad (24)$$

In the case of accretion onto a stellar cluster, the distributed mass and the presence of multiple accretion sources will modify these profiles. We can generalise them as

$$V_{\text{rel}} \propto R^{-\eta}, \quad (25)$$

and

$$\rho \propto R^{-\zeta}, \quad (26)$$

under the constraint that the mass infall, $4\pi R^2 \rho V_{\text{rel}}$ decreases with decreasing radius, $\eta + \zeta \leq 2$. we have

$$\begin{aligned} \dot{M}_{*} &\propto V_{\text{rel}} \rho R_{\text{BH}}^2 \\ &\propto V_{\text{rel}} \rho \left(\frac{M_{*}}{V_{\text{rel}}^2} \right)^2 \\ &\propto \rho \frac{M_{*}^2}{V_{\text{rel}}^3} \\ &\propto g(t) R^{-\zeta} M_{*}^2 R^{3\eta} \\ &\propto g(t) M_{*}^2 R^{3\eta - \zeta}. \end{aligned} \quad (27)$$

As above, $g(t)$ includes the time-dependence of the homologically evolving cluster and R is the initial stellar position in the cluster. In the case where $3\eta - \zeta = 0$ as occurs for accretion onto a point mass, the accretion rates are independent of position in the cluster.

Assuming that the cluster maintains the same form ($3\eta - \zeta \approx \text{constant}$), solutions to equation(27) are

$$M_{*} = \frac{M_{*}(0)}{1 - \beta M_{*}(0)h(t)} \quad (28)$$

where $M_{*}(0)$ is the initial stellar mass, $h(t) = \int g(t)dt$, and β is basically the accretion clock which depends on the gas content and on $R^{3\eta - \zeta}$ but not on time. The primary difference between this case and the preceding tidal-lobe accretion is the higher dependency on the stellar mass such that the initial mass is always important. This is the case for any accretion rate which depends on the stellar mass to a power greater than one.

The resulting mass spectrum from such an accretion rate was studied by Zinnecker (1982) and we follow his derivation here. As there is a direct correlation between initial and final mass, then there is a direct mapping from the initial mass spectrum to the final one,

$$F(M_{*})dM_{*} = F(M_{*}(0))dM_{*}(0). \quad (29)$$

Inverting equation(28) and inserting it into equation(29), as long as β is independent of the initial masses, we have

$$\begin{aligned} F(M_{*}) &= F(M_{*}(0)) \left(\frac{dM_{*}}{dM_{*}(0)} \right)^{-1} \\ &= F(M_{*}(0)) \left(\frac{d}{dM_{*}(0)} \frac{M_{*}(0)}{1 - \beta M_{*}(0)h(t)} \right)^{-1}, \\ &= F(M_{*}(0)) (1 - \beta M_{*}(0)h(t))^2, \\ &= F \left(\frac{M_{*}}{1 + \beta M_{*}h(t)} \right) \left(\frac{M_{*}(0)}{M_{*}} \right)^2. \end{aligned} \quad (30)$$

In the limit $\beta M_{*}h(t) \gg 1$ ($M_{*} \gg M_{*}(0)$) this gives

$$F(M_{*}) \propto M_{*}^{-2}, \quad (31)$$

and thus as long as there is an initial (small) range of stellar masses, the asymptotic limit of the mass spectrum is

$$dN \propto M_{*}^{-2} dM_{*}. \quad (32)$$

This is somewhat complicated if there is a correlation between the initial masses and radii in the cluster. In this

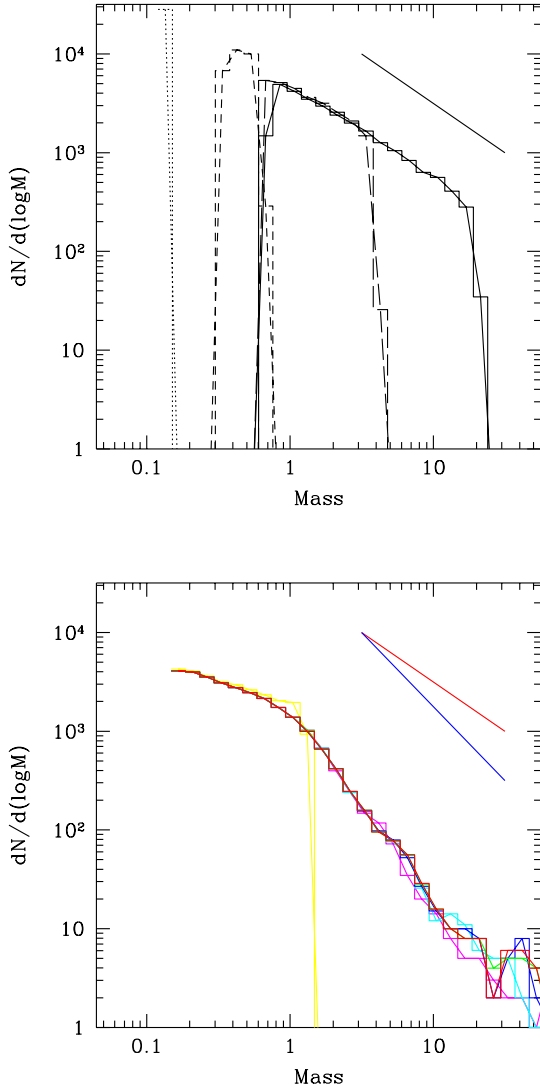


Figure 2. Simulated IMFs for a combined 28 clusters containing 1000 stars each are plotted in log mass bins. The clusters are assumed to have stellar dominated potentials and accrete according to either equation(27) with no spatial dependence (upper panel) or equation(33) for an initially mass-segregated cluster (lower panel). The stars are in a $n \propto R^{-2}$ configuration and are initially a delta function in mass (upper panel) or the expected $\gamma = -3/2$ ($\Gamma = -1/2$) mass spectrum from tidal-lobe accretion (where Salpeter is $\gamma = -2.35$). The higher-mass stars develop the steeper $\gamma = -2$ and $\gamma = -5/2$ ($\Gamma = -3/2$) mass spectra due to the accretion. The solid lines demonstrate the $\gamma = -2$ and $\gamma = -2.5$ slopes.

case β is dependent on $M_*(0)$ and we cannot derive an analytical expression for the resulting mass spectrum. In the case where the incoming mass distribution is from the tidal-lobe accretion, then from §3.1 we have an expression for the initial mass-radius correlation (equation 17). Using this, we can generate a mass spectrum from accretion for a cluster in a $n \propto R^{-2}$ configuration. Numerical simulations of accretion in stellar dominated clusters have values of $\eta = 1/3$ and $\zeta = 3/2$ (Bonnell et al. 2000). Equation (27) then becomes

$$\dot{M}_* \propto M_*^2 R^{-\frac{1}{2}}. \quad (33)$$

Figure 2 shows the resultant IMF for clusters accreting from an initial delta function mass distribution and those with an initially $M_*^{-3/2}$ mass spectrum that accretes according to equation (33). In the former case, the stars, in a $n \propto r^{-2}$ distribution, accrete with a spatially-independent accretion rate ($\dot{M}_* \propto M_*^2$). These clusters develop an M_*^{-2} mass spectrum. In contrast, with the initial mass segregation, the IMF develops into a steeper ($\gamma \approx -2.5$) IMF as the stars accrete in the stellar dominated regime. This is somewhat steeper than the analytical M_*^{-2} mass spectrum due to the initial correlation between stellar mass and position in the cluster.

We expect stellar dominated clusters to accrete towards a mass spectrum with asymptotic limits of $-2.5 \lesssim \gamma \leq -2$. This mass spectrum is expected for the higher mass stars as it is they that are located in the centre of the cluster and have attained a higher mass due to their previous accretion in the gas dominated regime. Clusters that have mass distributions that are uncorrelated with cluster position going into the stellar dominated phase result in mass spectra of $\gamma \approx -2$ whereas those that are mass segregated initially will have slightly steeper mass spectra $\gamma \approx -2.5$.

It is important to note that the above derivation relies upon all the stars stopping their accretion at the same time, as the final masses are a strong function of the time (equation 28). This should not be too strong a limitation as in the stellar dominated potential the accretion timescale must be much longer than the local crossing time as $M_{\text{gas}} \ll M_{\text{stars}}$. In a rich young stellar cluster, gas removal is due to the presence of massive stars. These stars ionise the gas such that the sound speed (≈ 10 km/s) is comparable to or greater than the velocity dispersion. Thus the gas should be removed on a timescale shorter than or comparable to the crossing time, and all the stars in the core should stop accreting quasi-simultaneously. If this is not the case, then the resulting mass spectrum will exhibit a local maximum corresponding to stars that are just outside the cleared region.

In summary, we expect that the combination of a gas dominated and a stellar dominated regimes and the different accretion physics operating in each, results in a two power-law IMF. The lower-mass stars have a shallower ($\gamma \approx -1.5$) slope as their mass accumulation is dominated by tidal-lobe accretion whereas the higher mass stars have a steeper ($-2 \geq \gamma \gtrsim -2.5$) slope as their mass accumulation is dominated by Bondi-Hoyle accretion in the stellar dominated core.

4 SIMULATED CLUSTER IMFS

In order to explore the relevance of the asymptotic limits for the mass spectrum, we performed a number of simulations of accretion onto a cluster of 1000 stars. The stars are initially of equal mass ($0.1M_\odot$) and are embedded in gas which comprises 91 per cent of the total cluster mass. The gas is cold such that it contains 1000 Jeans masses,

$$M_J = \left(\frac{5R_g T}{2G\mu} \right)^{3/2} \left(\frac{4}{3}\pi\rho \right)^{-1/2}, \quad (34)$$

where ρ is the gas density, T is the gas temperature, R_g is the gas constant, G is the gravitational constant, and μ is the mean molecular weight. The simulations were per-

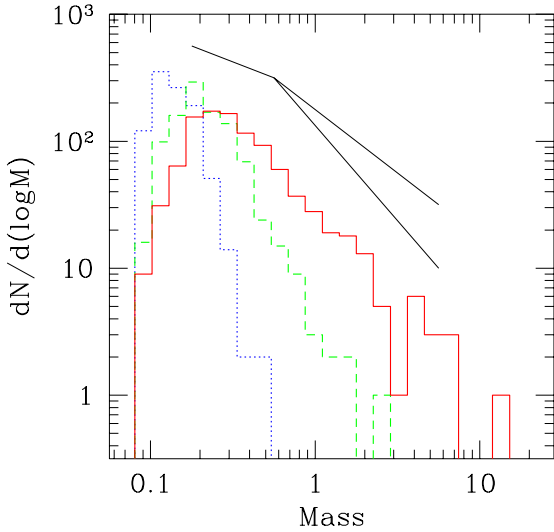


Figure 3. Histograms of the resultant mass spectra are plotted (in log mass bins) for a cluster containing 1000 stars that initially comprise 10 per cent of the total mass. The mass spectra are presented at three different times (dotted line, $t = 0.5t_{\text{ff}}$; dashed line, $t = 0.8t_{\text{ff}}$; and solid line, $t = 0.96t_{\text{ff}}$). The solid lines denote the expected slopes of $\gamma = -3/2$ for low-mass stars and $\gamma = -5/2$ for high-mass stars.

formed with a hybrid N-body SPH code (Bate, Bonnell & Price 1995) which uses standard SPH particles to model the gas and sink-particles to model the stars (for more details see also Bonnell et al. 2000). These sink-particles interact only gravitationally with the rest of the cluster and by accreting gas particles that come within their sink radius. This sink or accretion radius was taken to be the smaller of the tidal-lobe radius, the Bondi-Hoyle radius or the stellar separation. In addition, gas particles can only be accreted if they are bound to the star. The simulations were performed with either 9000 or 90000 SPH particles. The low-resolution simulations resulted in an excess of stars in the lowest (initial) mass bins as they were not able to resolve the low accretion rates involved. The higher-resolution simulations resolved the accretion onto all stars and both low and high-resolution simulations resulted in similar high-mass mass-spectra.

Both the stellar and gas distribution are initially uniform but collapse down towards a centrally condensed distribution. Gas is accreted by the stars and removed from the simulation. As the gas is accreted preferentially near the centre once a power-law density profile is established ($\rho \propto R^{-2}$), the stars soon dominate the potential there. The gas must then infall from further out in the cluster. The simulations result in mass spectra that are broadly consistent with our analytical expectations. The low-mass stars that accrete their mass during the gas dominated phase display shallow ($\gamma \approx -3/2$) mass spectra whereas the high-mass stars that accrete the majority of their mass during the stellar dominated phase display steeper ($-2.5 \lesssim \gamma \leq -2$) mass spectra. As the clusters are initially uniform and cold, only the end of the simulations develop a power-law density profile and that just before entering the stellar dominated regime. Because of this, the expected low-mass mass spectrum does not extend over a large mass range.

In Figure 3, we plot the resultant mass function for one of the higher resolution simulations, (performed with 90000

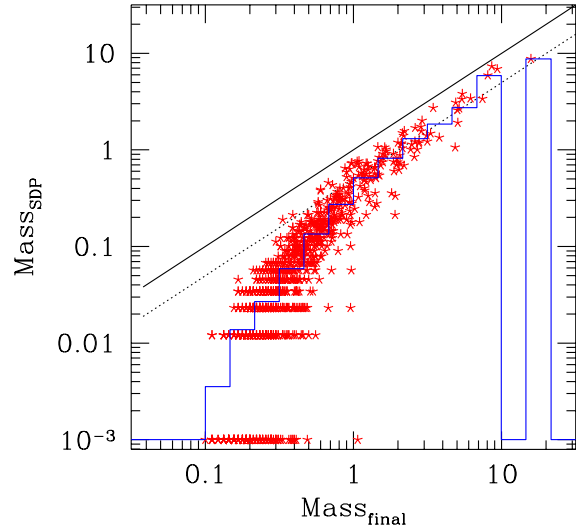


Figure 4. The mass accreted during the stellar-dominated phase, Mass_{SDP} , is plotted against total stellar mass. High mass stars derive the vast majority of their mass from the accretion in a stellar dominated potential whereas the majority of low-mass stars accumulate their mass predominantly in the gas-dominated phase. The continuous line represents where stars would lie if all their mass was accreted during the stellar-dominated phase whereas the dotted line represents where stars would lie if half of their final mass was accreted during this phase. The solid histogram gives the mean mass accreted in the stellar dominated potential as a function of final stellar mass.

SPH particles) at three different times during the evolution. The mass spectrum increases in breadth with time and develops into a power-law for the high-mass stars. The low-mass mass spectrum is broadly consistent with tidal-lobe accretion in a mostly uniform cloud, although only over a small range in mass. Due to the uniform initial conditions, only a fraction of the stars experience the power-law density profile before entering the stellar-dominated phase. This region would extend further in mass if the cluster was initially centrally condensed when accretion begins. At later times, the high-mass mass spectrum converges to a slope between $\gamma = -2$ and $\gamma = -2.5$ consistent with the accretion during the stellar dominated phase, and to the Salpeter slope of $\gamma = -2.35$.

4.1 Accretion dynamics

In order ascertain whether we are correct in our interpretation of a two-power law IMF resulting from accretion in gas-dominated and stellar-dominated regimes, we evaluated how much of the eventual stellar mass was added in each regime. Figure 4 plots the amount of mass accumulated by each star during the stellar-dominated phase against the final stellar mass. High-mass stars accumulate the majority of their mass during this phase whereas most of the low-mass stars only accrete a small fraction of their mass during this phase. The break between the two regimes occurs at approximately the same final mass ($\approx 1M_{\odot}$) where the mass function displays a break between the two slopes. This supports the assertion that the two different power-laws in the IMF derive from different physical regimes which affect how the stars accrete. The low-mass stars derive their mass from tidal-lobe accre-

tion during the gas-dominated regime whereas the high-mass stars derive the majority of their mass from a Bondi-Hoyle type accretion that occurs in the inner parts of the cluster where the potential is dominated by the stars themselves.

5 DISCUSSION

In addition to producing the two power-law mass spectrum, competitive accretion naturally results in a certain degree of mass segregation. This arises due to the accretion in the gas-dominated phase where there is a strong correlation between accretion rate, and thus the final mass, and position in the cluster (see equations(16) and (20)). This direct correlation between the final mass and position in the cluster neglects variations in the initial masses and the relative movements of the stars due to their interactions. If the cluster is mass segregated entering the stellar dominated phase, then the $\dot{M}_* \propto M_*^2$ implies that the mass segregation will persist. Simulations of accretion in clusters show that the mass segregation does result but that there is not a one to one correlation between mass and radius (Bonnell et al. 2000). In fact, low-mass stars are located throughout the cluster, including in the core, but the high-mass stars are predominantly located in the central regions as is found in young stellar clusters such as the ONC (Hillenbrand 1997).

It is also worth noting that although the models presented here are meant to consider accretion onto young stars, they are equally appropriate for the growth of clumps in a molecular cloud. As the clumps evolve towards gravitational instability, they will accrete from the surrounding gas and this accretion will be governed by the physics described here. Thus, for example, the clump mass-function found by Motte, André & Neri (1998) for the ρ Oph molecular cloud could be due to the accretion by the pre-stellar clumps as the whole system collapses down to form a cluster. The observed $\gamma = -3/2$ slope would imply that the whole system is in a $\rho \propto R^{-2}$ density configuration and is subvirial (dominated by the diffuse gas not in the clumps). The steeper slope found by Motte et al. (1998) at the high-mass end of the mass spectrum can be interpreted as arising from a region of near-uniform gas density. A test of such a possibility is to estimate the degree of mass segregation of the clumps in this pre-stellar cluster system.

Finally, it is possible that the mass spectrum for massive stars, $M_* \gtrsim 10M_\odot$, is significantly different than that for lower mass stars if they do not form in a similar fashion. If massive stars cannot accrete above $10M_\odot$ due to the effect of radiation pressure on the infalling dust (Yorke & Krügel 1977; Yorke 1993) but form through a merger process in a dense core (Bonnell et al. 1998) then the expected mass spectrum could be significantly different from that presented here.

6 CONCLUSIONS

Competitive accretion in young stellar clusters results in a two power-law mass spectrum with a slope of $\gamma \approx -3/2$ for low-mass stars and a steeper slope of $-2 \geq \gamma \gtrsim -2.5$ for high-mass stars. The different slopes are due to whether the gas

or the stars dominate the cluster potential. When gas dominates the cluster potential, the accretion rates are given by a tidal-lobe accretion radius and results in a $dN \propto M_*^{-3/2} dM_*$ mass spectrum in an isothermal sphere distribution. The shallower density profile in the central regions implies a steeper mass spectrum, $3/2 \geq \gamma \gtrsim -4$. Once the stars have accreted enough to dominate the potential, which occurs from the inside out, the appropriate accretion radius is the Bondi-Hoyle radius. When this happens the strong dependence of the accretion rate on stellar mass $\dot{M}_* \propto M_*^2$ results in a mass spectrum of $dN \propto M_*^{-2} dM_*$ to $dN \propto M_*^{-2.5} dM_*$.

Simulations of accretion in clusters containing 1000 stars result in mass spectra broadly consistent with these analytic estimates. The high-mass stars are confirmed to accumulate the majority of their mass in a stellar-dominated potential. Lastly, competitive accretion in clusters naturally results in mass segregation as the accretion rates are higher near the cluster centre during the gas dominated phase.

7 ACKNOWLEDGEMENTS

We thank Hans Zinnecker for useful discussions and continual enthusiasm. IAB acknowledges support from a PPARC advanced fellowship.

REFERENCES

- Adams F. C., Fattuzzo M., 1996, ApJ, 464, 256
 Bate M. R., Bonnell I. A., Price N. M., 1995, 277, 362
 Binney J., Tremaine S., 1987, in *Galactic Dynamics*, Princeton University.
 Bondi H., Hoyle F., 1944, MNRAS, 104, 273
 Bonnell I. A., Bastien P., 1992, ApJ, 401, 654
 Bonnell I. A., Bate M. R., Clarke C. J., Pringle J. E., 1997, MNRAS, 285, 201
 Bonnell I. A., Bate M. R., Clarke C. J., Pringle J. E., 2000, MNRAS, submitted
 Bonnell I. A., Bate M. R., Zinnecker H., 1998, MNRAS, 298, 93
 Bonnell I. A., Davies M.B., 1998, MNRAS, 295, 691
 Boss A. P., 1986, ApJS, 62, 519
 Burkert A., Bodenheimer P., 1993, MNRAS, 264, 798
 Clarke C.J., 1998, in *The Stellar Initial Mass Function*, eds G. Gilmore and D. Howell (ASP Vol 142), p. 189
 Clarke C.J., Bonnell I.A., Hillenbrand L.A., 2000, in *Protostars and Planets IV*, eds V. Mannings, A. P. Boss and S. S. Russell (Tucson: University of Arizona Press), p. 151
 Elmegreen B. G., 1997, ApJ, 486, 944
 Foster P. N., Chevalier R. A., 1993, ApJ, 416, 303
 Frank J., King A., Raine D., 1985. *Accretion Power in Astrophysics*, (Cambridge University Press), p. 51.
 Hillenbrand L. A., 1997, AJ, 113, 1733
 Hillenbrand L. A., Carpenter J. 2000, ApJ, 540, 236
 Hillenbrand L. A., Hartmann L., 1998, ApJ, 492, 540
 Hunter C., 1977, AppJ, 218, 834
 Kennicutt R. C., 1998, in *The Stellar Initial Mass Function*, eds G. Gilmore and D. Howell (ASP Vol 142), p. 1
 Klessen R., Burkert A., Bate M. R., 1998, ApJL, 501, L205
 Kroupa P., Tout C., Gilmore G., 1990, MNRAS, 244, 76
 Lada C., 1991, in *The Physics of Star Formation and Early Stellar Evolution*, eds C. J. Lada, N. D. Kylafis, Kluwer, p. 329
 Lada E. A., Depoy D. L., Evans N. J. Gatlley I. 1991, ApJ, 371, 171
 Lada E., Strom S., Myers P., 1993, in *Protostars and Planets III*, eds E. Levy, J. Lunine, University of Arizona, p. 245

- Larson R. B., 1969, MNRAS, 145, 271
Larson R. B., 1978, MNRAS, 184, 69
Larson R. B., 1992, MNRAS, 256, 641
Leitherer C., 1998, in *The Stellar Initial Mass Function*, eds G. Gilmore and D. Howell (ASP Vol 142), p. 61
Lynden-Bell D., 1967, MNRAS, 136, 101
Meyer M. R., Adams F. C., Hillenbrand L. A., Carpenter J. M., Larson R. B., 2000 in *Protostars and Planets IV*, eds V. Mannings, A. P. Boss and S. S. Russell (Tucson: University of Arizona Press), in press
Meyer M., Lada E. A., 1999, in *The Orion Nebula Revisited*, M. McCaugrean and A. Burkert (eds), in press
Motte F., André P., Neri R., 1998, A&A, 336, 150
Paczynski, B., 1971, ARA&A, 9, 183
Ruffert M., 1996, A&A, 311, 817
Scalo J. M., 1986, Fund. Cosmic Phys., 11, 1
Scalo J. M., 1998, in *The Stellar Initial Mass Function*, eds G. Gilmore and D. Howell (ASP Vol 142), p. 201
Shu F., 1977, ApJ, 214, 488
Silk J., 1977, 214, 718
Yorke H. W. 1993, in *Massive Stars: Their Lives in the interstellar Medium*, eds. J. Cassinelli, E. Churchwell, ASP Conf. Ser. 35:45–55.
Yorke H. W., Krügel E., 1977, A&A, 54, 183
Zinnecker H., 1982 in *Symposium on the Orion Nebula to Honour Henry Draper*, eds A. E. Glassgold et al., New York Academy of Sciences, p. 226